

Higher-Order Stability Analysis of Imperfect Laminated Piezo-Composite Plates on Elastic Foundations Under Electro-Thermo-Mechanical Loads

B. Mirzavand^{*}, M. Bohlooly

Faculty of New Sciences and Technologies, University of Tehran, Tehran, Iran

Received 5 June 2019; accepted 4 August 2019

ABSTRACT

This article provides a fully analytical approach for nonlinear equilibrium path of rectangular sandwich plates. The core of structure is made of symmetric cross-ply laminated composite and the outer surfaces are piezoelectric actuators, which perfectly bonded to inner core. The structure is subjected to electro-thermo-mechanical loads simultaneously. One side of plate is rested on Pasternak type elastic foundation. The equilibrium equations of plate are derived based on the higher-order shear deformation theory of Reddy taking into account initial geometrical imperfection, nonlinear strain-displacement relations of von-Karman, temperature dependent properties, and different types of boundary conditions. Some numerical examples are presented to verify the accuracy of the proposed formulation. The effects of various parameters such as voltage on actuators, elastic foundation, imperfection, and pre-load condition on the buckling and post buckling behaviors are studied. As an important finding of current research, there may be exists bifurcation point for imperfect plates by applying voltage on actuators.

© 2019 IAU, Arak Branch. All rights reserved.

Keywords: Imperfection; Sandwich; Elastic foundation; Galerkin; HSDT.

1 INTRODUCTION

ISOTROPIC materials gradually replaced by fibrous composite materials in the industries. In order to extremely usage of these materials, researchers are constantly seeking new ways to improve mechanical behavior of composites, in which sandwich piezo-composite material is one of the ways to increase of durability of bare composites. Furthermore, elastic foundations have positive influence on the buckling and post buckling behavior of structures. A lot of real engineering problems can be modeled as moderately thick plates and shells on elastic foundations such as oil, gas, water, and sewage pipelines in the seabed and/or ground. For isotropic materials, the post buckling studies of plates on Winkler and or Pasternak type elastic foundations can be found in [1-3]. In the case of laminated composites, Shen [4-6] and Shen and Li [7] investigated effect of the Pasternak elastic foundation

^{*}Corresponding author.

E-mail address: mirzavand@ut.ac.ir (B. Mirzavand).

on buckling and post buckling of imperfect laminated composite plates under thermal, mechanical, and combined loads using perturbation technique. Yang and Zhang [8] presented mechanical post buckling of imperfect laminated plates on Pasternak elastic foundation using a semi-analytical approach based on classical theory. Singh et al. [9] and Singh and Lal [10] studied post buckling of laminated composite plates with random system properties on elastic foundation using finite element method based on higher-order theory. Pandey et al. [11] presented buckling and post buckling response of laminated composite plates resting on elastic foundation utilizing finite double Chebyshev polynomials based on higher-order theory. Compared to the several investigations on post buckling behavior of laminated composite plates for example [12-16], there exist limited studies on post buckling of sandwich piezo laminated plates. Oh et al. [17] presented post buckling and vibration of piezoelectric-composite plates by nonlinear finite element equations based on the layer wise plate theory. In their study, the piezoelectric layers fully and partially bonded to composite. Shen [18] studied thermal post buckling of shear-deformable laminated plates with piezoelectric actuators. In that study, a mixed Galerkin perturbation technique was employed to determine thermal critical loads and post buckling equilibrium paths, and the material properties were assumed independent of the temperature. In the same year, Shen [19] investigated electro-thermo-mechanical buckling and post buckling of shear-deformable [piezoelectric/composite/piezoelectric], using a mixed Galerkin perturbation technique, and temperature-independent material properties. Varelis and Saravanos [20] analyzed coupled electrical and mechanical fields together with finite element method for predicting of buckling and post buckling response of laminated composite plates with piezoelectric actuators and sensors, which included nonlinear effects due to large rotations and stress stiffening. In their work, nonlinear equations formulated using mixed-field shear-layer wise kinematic assumptions, then linearized and solved using an incremental-iterative method based on the Newton-Raphson technique. Recently, Bohlooly and Mirzavand [21] presented buckling and post buckling of imperfect very thin laminated composite plates with surface mounted and embedded piezoelectric actuators under electro-thermo-mechanical loads and various boundary conditions. In that study, the formulation is based on the classical laminated plate theory and then using Galerkin procedure, the resulting equations are solved to obtain fully closed form expressions for nonlinear equilibrium paths. This survey in the literature reveals that, there is no any presentation for electro-thermo-mechanical buckling and post buckling of moderately thick [piezoelectric/composite/piezoelectric] plates resting on elastic foundations. The novelty of this paper is to obtain fully closed form solutions for post buckling of shear deformable sandwich piezo laminated plates, importing elastic foundation, which could be useful from the engineering's point of view.

In recent years, different plates and shells surrounded by the Pasternak elastic foundation began to be investigated in a variety of industrial applications. In this context, Abdollahian et al. [22] and Ghorbanpour Arani et al. [23] studied electro-thermo-mechanical wave propagation and buckling in an embedded armchair double and three-walled boron nitride on Pasternak foundation. Also, Ghorbanpour Arani et al. [24,25] worked on nonlinear vibration analysis of bioliquid-filled microtubules embedded in cytoplasm and embedded smart composite micro tube conveying fluid with Pasternak elastic foundation. The effects of Pasternak type elastic foundation on the post buckling and deflection response of thin imperfect piezoelectric-composite plates are investigated by Bohlooly and Mirzavand [26].

It can be seen in previous work [21], a number of mechanical, electro-thermal, and electro-thermo-mechanical post buckling of plate in the absence of elastic foundation are verified with known literature. This paper extends the previous work to investigate closed form expressions for buckling and post buckling behavior of moderately thick sandwich composite plates with surface mounted piezoelectric actuators resting on Pasternak type elastic foundation under mechanical, thermal, electrical, and combined loads based on third order shear deformation theory of Reddy with von-Karman nonlinear kinematic relations. Initial geometrical imperfections are also accounted, and by applying Galerkin procedure, the resulting equations are solved to obtain closed form expressions for nonlinear equilibrium paths. Temperature dependency of thermo-mechanical properties is considered. Three cases of boundary conditions are investigated. Effects of elastic foundation parameters, initial geometrical imperfections, in-plane compressive loading, temperature dependency and independency of properties, and electrical loading are discussed. Results for various states are verified with the known data in the literature.

2 GOVERNING EQUATIONS

Consider a rectangular sandwich plate of length a , width b , and total thickness h as shown in Fig. 1. The plate is composed of perfectly bonded orthotropic cross-ply laminas of total thickness $2h_c$, and each piezoelectric films of thickness h_a , perfectly bonded on the top and bottom surfaces as actuators. Rectangular Cartesian coordinates

(x, y, z) are assumed for derivations, the angle of fibers θ in laminated composites is expressed with reference to the x coordinate, and the structure is symmetrically laminated.

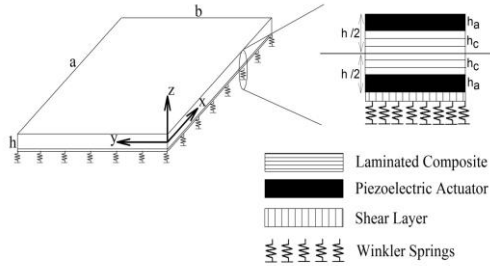


Fig.1
The geometry and structure of the piezo laminated sandwich plate on elastic foundation.

In this study, third order shear deformation plate theory of Reddy is used to establish governing equations and determine the nonlinear equilibrium path of the sandwich plate. According to this theory, the displacement field is assumed as [27]

$$\begin{aligned}
 u(x, y, z) &= u_0(x, y) + z \phi_x(x, y) - c_1 z^3 [\phi_x(x, y) + w_{0,x}(x, y)] \\
 v(x, y, z) &= v_0(x, y) + z \phi_y(x, y) - c_1 z^3 [\phi_y(x, y) + w_{0,y}(x, y)] \\
 w(x, y, z) &= w_0(x, y)
 \end{aligned}
 \tag{1}$$

Here (u, v, w) are the plate displacements parallel to the coordinates (x, y, z) and a comma indicates the partial derivative. The components (u_0, v_0, w_0) represent the displacements on the middle plane ($z = 0$) of the plate, ϕ_x and ϕ_y are the middle plane rotations of transverse normal about the y and x axes, respectively. Here $c_1 = 4/(3h^2)$, where the traction-free boundary conditions on the top and bottom faces of the piezo-laminated plate are satisfied.

The nonlinear strain-displacement relations of von-Karman including initial geometrical imperfection $w^*(x, y)$ are expressed as: [28]

$$\begin{aligned}
 \epsilon_{xx} &= u_{,x} + \frac{1}{2} w_{,x}^2 + w^*_{,x} w_{,x} \\
 \epsilon_{yy} &= v_{,y} + \frac{1}{2} w_{,y}^2 + w^*_{,y} w_{,y} \\
 \gamma_{xy} &= u_{,y} + v_{,x} + w_{,x} w_{,y} + w^*_{,x} w_{,y} + w^*_{,y} w_{,x} \\
 \gamma_{yz} &= v_{,z} + w_{,y} \\
 \gamma_{zx} &= u_{,z} + w_{,x}
 \end{aligned}
 \tag{2}$$

where ϵ_{xx} and ϵ_{yy} are the normal strains and γ_{xy} , γ_{yz} , and γ_{zx} are the shear strains.

Substituting Eq. (1) into the nonlinear strain-displacement relations (2) results the kinematic relations as:

$$\begin{Bmatrix} \epsilon_{xx} \\ \epsilon_{yy} \\ \gamma_{yz} \\ \gamma_{zx} \\ \gamma_{xy} \end{Bmatrix} = \begin{Bmatrix} \epsilon_{xx}^{(0)} \\ \epsilon_{yy}^{(0)} \\ \gamma_{yz}^{(0)} \\ \gamma_{zx}^{(0)} \\ \gamma_{xy}^{(0)} \end{Bmatrix} + z \begin{Bmatrix} \epsilon_{xx}^{(1)} \\ \epsilon_{yy}^{(1)} \\ \gamma_{yz}^{(1)} \\ \gamma_{zx}^{(1)} \\ \gamma_{xy}^{(1)} \end{Bmatrix} + z^2 \begin{Bmatrix} \epsilon_{xx}^{(2)} \\ \epsilon_{yy}^{(2)} \\ \gamma_{yz}^{(2)} \\ \gamma_{zx}^{(2)} \\ \gamma_{xy}^{(2)} \end{Bmatrix} + z^3 \begin{Bmatrix} \epsilon_{xx}^{(3)} \\ \epsilon_{yy}^{(3)} \\ \gamma_{yz}^{(3)} \\ \gamma_{zx}^{(3)} \\ \gamma_{xy}^{(3)} \end{Bmatrix}
 \tag{3}$$

where

$$\begin{aligned}
 \begin{Bmatrix} \varepsilon_{xx}^{(0)} \\ \varepsilon_{yy}^{(0)} \\ \gamma_{yz}^{(0)} \\ \gamma_{zx}^{(0)} \\ \gamma_{xy}^{(0)} \end{Bmatrix} &= \begin{Bmatrix} u_{0,x} + \frac{1}{2}w_{0,x}^2 + w_{0,x}^* w_{0,x} \\ v_{0,y} + \frac{1}{2}w_{0,y}^2 + w_{0,y}^* w_{0,y} \\ \phi_y + w_{0,y} \\ \phi_x + w_{0,x} \\ u_{0,y} + v_{0,x} + w_{0,x} w_{0,y} + w_{0,x}^* w_{0,y} + w_{0,x} w_{0,y}^* \end{Bmatrix}, \quad \begin{Bmatrix} \varepsilon_{xx}^{(1)} \\ \varepsilon_{yy}^{(1)} \\ \gamma_{yz}^{(1)} \\ \gamma_{zx}^{(1)} \\ \gamma_{xy}^{(1)} \end{Bmatrix} = \begin{Bmatrix} \phi_{x,x} \\ \phi_{y,y} \\ 0 \\ 0 \\ \phi_{x,y} + \phi_{y,x} \end{Bmatrix} \\
 \begin{Bmatrix} \varepsilon_{xx}^{(2)} \\ \varepsilon_{yy}^{(2)} \\ \gamma_{yz}^{(2)} \\ \gamma_{zx}^{(2)} \\ \gamma_{xy}^{(2)} \end{Bmatrix} &= -3c_1 \begin{Bmatrix} 0 \\ 0 \\ \phi_y + w_{0,y} \\ \phi_x + w_{0,x} \\ 0 \end{Bmatrix}, \quad \begin{Bmatrix} \varepsilon_{xx}^{(3)} \\ \varepsilon_{yy}^{(3)} \\ \gamma_{yz}^{(3)} \\ \gamma_{zx}^{(3)} \\ \gamma_{xy}^{(3)} \end{Bmatrix} = -c_1 \begin{Bmatrix} \phi_{x,x} + w_{0,xx} \\ \phi_{y,y} + w_{0,yy} \\ 0 \\ 0 \\ \phi_{x,y} + \phi_{y,x} + 2w_{0,xy} \end{Bmatrix}
 \end{aligned} \tag{4}$$

The load-deflection relation of Pasternak foundation is defined as: [29,30]

$$q_{ef} = K_1 w_0 - K_2 (w_{0,xx} + w_{0,yy}) \tag{5}$$

where q_{ef} the foundation reaction per unit area is, K_1 Winkler foundation modulus, and K_2 is the shear layer foundation stiffness of Pasternak model.

The constitutive equations for the k^{th} ply of laminated composite ($1 < k < N$), taking into account the thermal effects are given by [27]

$$\begin{Bmatrix} \sigma_{xx} \\ \sigma_{yy} \\ \tau_{yz} \\ \tau_{zx} \\ \tau_{xy} \end{Bmatrix}_k = \begin{Bmatrix} \bar{Q}_{11} & \bar{Q}_{12} & 0 & 0 & \bar{Q}_{16} \\ \bar{Q}_{12} & \bar{Q}_{22} & 0 & 0 & \bar{Q}_{26} \\ 0 & 0 & \bar{Q}_{44} & \bar{Q}_{45} & 0 \\ 0 & 0 & \bar{Q}_{45} & \bar{Q}_{55} & 0 \\ \bar{Q}_{16} & \bar{Q}_{26} & 0 & 0 & \bar{Q}_{66} \end{Bmatrix}_k \begin{Bmatrix} \varepsilon_{xx} - \alpha_x \Theta \\ \varepsilon_{yy} - \alpha_y \Theta \\ \gamma_{yz} \\ \gamma_{zx} \\ \gamma_{xy} - \alpha_{xy} \Theta \end{Bmatrix}_k \tag{6}$$

and for the piezoelectric layers [27]

$$\begin{Bmatrix} \sigma_{xx} \\ \sigma_{yy} \\ \tau_{yz} \\ \tau_{zx} \\ \tau_{xy} \end{Bmatrix} = \begin{Bmatrix} Q_{11}^a & Q_{12}^a & 0 & 0 & 0 \\ Q_{12}^a & Q_{22}^a & 0 & 0 & 0 \\ 0 & 0 & Q_{44}^a & 0 & 0 \\ 0 & 0 & 0 & Q_{55}^a & 0 \\ 0 & 0 & 0 & 0 & Q_{66}^a \end{Bmatrix} \begin{Bmatrix} \varepsilon_{xx} - \alpha_x^a \Theta \\ \varepsilon_{yy} - \alpha_y^a \Theta \\ \gamma_{yz} \\ \gamma_{zx} \\ \gamma_{xy} - \alpha_{xy}^a \Theta \end{Bmatrix} - \begin{Bmatrix} 0 & 0 & e_{31} \\ 0 & 0 & e_{32} \\ 0 & e_{24} & 0 \\ e_{15} & 0 & 0 \\ 0 & 0 & 0 \end{Bmatrix} \begin{Bmatrix} E_x \\ E_y \\ E_z \end{Bmatrix} \tag{7}$$

where σ_{xx} and σ_{yy} are the normal stresses and τ_{xy} , τ_{yz} , and τ_{zx} are the shear stresses, Θ is the temperature rise from a reference temperature corresponding to zero thermal strain, α_x , α_y , α_{xy} , α_x^a , α_y^a , and α_{xy}^a are the coefficients of thermal expansion, \bar{Q}_{ij} , Q_{ij}^a ($i, j = 1, 2, 4, 5, 6$) are the elastic stiffness, e_{31} , e_{32} , e_{24} , and e_{15} are piezoelectric stiffness, E_x , E_y , and E_z are electric field components and letters "a" means actuator. The coefficients of thermal expansion, elastic stiffness, and piezoelectric stiffness are provided in detail in Appendix A. In addition, the electric field components are given by [18,21,31]

$$E_x = E_y = 0, E_z = \frac{V^a}{h_a} \tag{8}$$

where V_a is the applied voltage across the thickness of a piezoelectric layer.

The stress resultants are related to the stresses by the equations [32]

$$\begin{Bmatrix} N_x & M_x & P_x \\ N_y & M_y & P_y \\ N_{xy} & M_{xy} & P_{xy} \end{Bmatrix} = \int_{-h_c-h_a}^{+h_c+h_a} \begin{Bmatrix} \sigma_{xx} \\ \sigma_{yy} \\ \tau_{xy} \end{Bmatrix} (1, z, z^3) dz, \quad \begin{Bmatrix} Q_y & R_y \\ Q_x & R_x \end{Bmatrix} = \int_{-h_c-h_a}^{+h_c+h_a} \begin{Bmatrix} \tau_{yz} \\ \tau_{zx} \end{Bmatrix} (1, z^2) dz \quad (9)$$

Using the constitutive Eqs. (6, 7), the stress resultants are found to be

$$\begin{aligned} \begin{Bmatrix} N_x & M_x & P_x \\ N_y & M_y & P_y \\ N_{xy} & M_{xy} & P_{xy} \end{Bmatrix} &= \begin{Bmatrix} Q_{11}^a & Q_{12}^a & 0 \\ Q_{12}^a & Q_{22}^a & 0 \\ 0 & 0 & Q_{66}^a \end{Bmatrix} \begin{Bmatrix} \varepsilon_{xx}^{(0)} \\ \varepsilon_{yy}^{(0)} \\ \gamma_{xy}^{(0)} \end{Bmatrix} (I_1, 0, 0) + \begin{Bmatrix} \varepsilon_{xx}^{(1)} \\ \varepsilon_{yy}^{(1)} \\ \gamma_{xy}^{(1)} \end{Bmatrix} (0, I_2, I_3) \\ &+ \begin{Bmatrix} \varepsilon_{xx}^{(3)} \\ \varepsilon_{yy}^{(3)} \\ \gamma_{xy}^{(3)} \end{Bmatrix} (0, I_3, I_4) - \begin{Bmatrix} e_{31} \\ e_{32} \\ 0 \end{Bmatrix} \frac{V_a}{h_a} (I_1, 0, 0) + [(A_{ij}, B_{ij}, E_{ij}) \begin{Bmatrix} \varepsilon_{xx}^{(0)} \\ \varepsilon_{yy}^{(0)} \\ \gamma_{xy}^{(0)} \end{Bmatrix} + (B_{ij}, D_{ij}, F_{ij}) \begin{Bmatrix} \varepsilon_{xx}^{(1)} \\ \varepsilon_{yy}^{(1)} \\ \gamma_{xy}^{(1)} \end{Bmatrix}] \\ &+ (E_{ij}, F_{ij}, J_{ij}) \begin{Bmatrix} \varepsilon_{xx}^{(3)} \\ \varepsilon_{yy}^{(3)} \\ \gamma_{xy}^{(3)} \end{Bmatrix} - \begin{Bmatrix} N_x^T & M_x^T & P_x^T \\ N_y^T & M_y^T & P_y^T \\ N_{xy}^T & M_{xy}^T & P_{xy}^T \end{Bmatrix} \quad i, j = 1, 2, 6 \\ \begin{Bmatrix} Q_y & R_y \\ Q_x & R_x \end{Bmatrix} &= \begin{Bmatrix} Q_{44}^a & 0 \\ 0 & Q_{55}^a \end{Bmatrix} \begin{Bmatrix} \gamma_{yz}^{(0)} \\ \gamma_{zx}^{(0)} \end{Bmatrix} (I_1, I_2) + \begin{Bmatrix} \gamma_{yz}^{(2)} \\ \gamma_{zx}^{(2)} \end{Bmatrix} (I_2, I_3) \\ &+ [(A_{ij}, D_{ij}) \begin{Bmatrix} \gamma_{yz}^{(0)} \\ \gamma_{zx}^{(0)} \end{Bmatrix} + (D_{ij}, F_{ij}) \begin{Bmatrix} \gamma_{yz}^{(2)} \\ \gamma_{zx}^{(2)} \end{Bmatrix}] \quad i, j = 4, 5 \end{aligned} \quad (10)$$

The thermal resultants can be described as: [27]

$$\begin{aligned} \begin{Bmatrix} N_x^T & M_x^T & P_x^T \\ N_y^T & M_y^T & P_y^T \\ N_{xy}^T & M_{xy}^T & P_{xy}^T \end{Bmatrix} &= \int_{-h_c-h_a}^{-h_c} \begin{Bmatrix} Q_{11}^a & Q_{12}^a & 0 \\ Q_{12}^a & Q_{22}^a & 0 \\ 0 & 0 & Q_{66}^a \end{Bmatrix} \begin{Bmatrix} \alpha_x^a \Theta \\ \alpha_y^a \Theta \\ \alpha_{xy}^a \Theta \end{Bmatrix} (1, z, z^3) dz \\ &+ \sum_{k=1}^N \int_{z_{k-1}}^{z_k} \begin{Bmatrix} \bar{Q}_{11} & \bar{Q}_{12} & \bar{Q}_{16} \\ \bar{Q}_{12} & \bar{Q}_{22} & \bar{Q}_{26} \\ \bar{Q}_{16} & \bar{Q}_{26} & \bar{Q}_{66} \end{Bmatrix}_k \begin{Bmatrix} \alpha_x \Theta \\ \alpha_y \Theta \\ \alpha_{xy} \Theta \end{Bmatrix}_k (1, z, z^3) dz + \int_{+h_c}^{+h_c+h_a} \begin{Bmatrix} Q_{11}^a & Q_{12}^a & 0 \\ Q_{12}^a & Q_{22}^a & 0 \\ 0 & 0 & Q_{66}^a \end{Bmatrix} \begin{Bmatrix} \alpha_x^a \Theta \\ \alpha_y^a \Theta \\ \alpha_{xy}^a \Theta \end{Bmatrix} (1, z, z^3) dz \end{aligned} \quad (11)$$

and stiffness components and inertias are given as: [27]

$$\begin{aligned} A_{ij}, B_{ij}, D_{ij}, E_{ij}, F_{ij}, J_{ij} &= \sum_{k=1}^N \begin{Bmatrix} \bar{Q}_{11} & \bar{Q}_{12} & \bar{Q}_{16} \\ \bar{Q}_{12} & \bar{Q}_{22} & \bar{Q}_{26} \\ \bar{Q}_{16} & \bar{Q}_{26} & \bar{Q}_{66} \end{Bmatrix}_k \left\{ (z_k - z_{k-1}), \frac{1}{2}(z_k^2 - z_{k-1}^2), \frac{1}{3}(z_k^3 - z_{k-1}^3), \right. \\ &\left. \frac{1}{4}(z_k^4 - z_{k-1}^4), \frac{1}{5}(z_k^5 - z_{k-1}^5), \frac{1}{7}(z_k^7 - z_{k-1}^7) \right\} \quad i, j = 1, 2, 6 \\ A_{ij}, D_{ij}, F_{ij} &= \sum_{k=1}^N \begin{Bmatrix} \bar{Q}_{44} & \bar{Q}_{45} \\ \bar{Q}_{45} & \bar{Q}_{55} \end{Bmatrix}_k \left\{ (z_k - z_{k-1}), \frac{1}{3}(z_k^3 - z_{k-1}^3), \frac{1}{5}(z_k^5 - z_{k-1}^5) \right\} \quad i, j = 4, 5 \\ I_1 &= 2h_a, \quad I_2 = \frac{2}{3}((h_c + h_a)^3 - (h_c)^3), \quad I_3 = \frac{2}{5}((h_c + h_a)^5 - (h_c)^5), \quad I_4 = \frac{2}{7}((h_c + h_a)^7 - (h_c)^7) \end{aligned} \quad (12)$$

The nonlinear equilibrium equations of the sandwich plate [piezoelectric/composite/ piezoelectric] resting on Pasternak type elastic foundation based on the higher-order shear deformation theory are [33]

$$\begin{aligned}
\frac{\partial}{\partial x} N_x + \frac{\partial}{\partial y} N_{xy} &= 0 \\
\frac{\partial}{\partial x} N_{xy} + \frac{\partial}{\partial y} N_y &= 0 \\
-K_1 w_0 + K_2 w_{0,xx} + K_2 w_{0,yy} + N_x (w_{0,xx} + w_{0,xx}^*) + 2N_{xy} (w_{0,xy} + w_{0,xy}^*) \\
+ N_y (w_{0,yy} + w_{0,yy}^*) + \left(\frac{\partial}{\partial x} Q_x + \frac{\partial}{\partial y} Q_y \right) & \\
-3c_1 \left(\frac{\partial}{\partial x} R_x + \frac{\partial}{\partial y} R_y \right) + c_1 \left(\frac{\partial^2}{\partial x^2} P_x + 2 \frac{\partial^2}{\partial x \partial y} P_{xy} + \frac{\partial^2}{\partial y^2} P_y \right) &= 0 \\
-Q_x + 3c_1 R_x + \left(\frac{\partial}{\partial x} M_x + \frac{\partial}{\partial y} M_{xy} \right) - c_1 \left(\frac{\partial}{\partial x} P_x + \frac{\partial}{\partial y} P_{xy} \right) &= 0 \\
-Q_y + 3c_1 R_y + \left(\frac{\partial}{\partial x} M_{xy} + \frac{\partial}{\partial y} M_y \right) - c_1 \left(\frac{\partial}{\partial x} P_{xy} + \frac{\partial}{\partial y} P_y \right) &= 0
\end{aligned} \tag{13}$$

By introducing the Airy stress function Φ as [21,33-35]: $N_x = \Phi_{,yy}$, $N_y = \Phi_{,xx}$, $N_{xy} = -\Phi_{,xy}$, the first and second equilibrium Eqs. (13) satisfy and the third, fourth, and fifth equilibrium equations reduce to one as:

$$\begin{aligned}
&\Phi_{,yy} (w_{0,xx} + w_{0,xx}^*) - 2\Phi_{,xy} (w_{0,xy} + w_{0,xy}^*) + \Phi_{,xx} (w_{0,yy} + w_{0,yy}^*) \\
&+ [(Q_{11}^a I_2 + D_{11}) - c_1 (Q_{11}^a I_3 + F_{11})] \phi_{x,xxx} \\
&+ [(Q_{12}^a I_2 + D_{12}) - c_1 (Q_{12}^a I_3 + F_{12})] + 2(Q_{66}^a I_2 + D_{66}) - 2c_1 (Q_{66}^a I_3 + F_{66}) \phi_{y,xyy} \\
&+ 3(D_{16} - c_1 F_{16}) \phi_{x,xyy} + (D_{16} - c_1 F_{16}) \phi_{y,xxx} - c_1 (Q_{11}^a I_3 + F_{11}) w_{0,xxxx} \\
&+ [-c_1 (Q_{12}^a I_3 + F_{12}) - 4c_1 (Q_{66}^a I_3 + F_{66}) - c_1 (Q_{12}^a I_3 + F_{12})] w_{0,xyy} \\
&- 4c_1 F_{16} w_{0,xyy} + 3(D_{26} - c_1 F_{26}) \phi_{y,yyy} \\
&+ [2(Q_{66}^a I_2 + D_{66}) - 2c_1 (Q_{66}^a I_3 + F_{66}) + (Q_{12}^a I_2 + D_{12}) - c_1 (Q_{12}^a I_3 + F_{12})] \phi_{x,yyy} \\
&- 4c_1 F_{26} w_{0,xyy} + [(Q_{22}^a I_2 + D_{22}) - c_1 (Q_{22}^a I_3 + F_{22})] \phi_{y,yyy} \\
&+ [D_{26} - c_1 F_{26}] \phi_{x,yyy} - c_1 (Q_{22}^a I_3 + F_{22}) w_{0,yyy} \\
&- K_1 w_0 + K_2 (w_{0,xx} + w_{0,yy}) - \frac{\partial^2}{\partial x^2} M_x^T - 2 \frac{\partial^2}{\partial x \partial y} M_{xy}^T - \frac{\partial^2}{\partial y^2} M_y^T = 0
\end{aligned} \tag{14}$$

On the other hand, the compatibility equation [21,35] of sandwich piezo laminated plates in terms of the Airy stress function Φ and the lateral displacement component w_0 may be obtained by using Eqs. (4) and (10), and also definition of Airy stress function as below

$$\begin{aligned}
&A Q_{11} (\Phi_{,yyyy} + \frac{\partial^2}{\partial y^2} N_x^T) + A Q_{12} (\Phi_{,xxyy} + \frac{\partial^2}{\partial y^2} N_y^T) + A Q_{16} (-\Phi_{,xyyy} + \frac{\partial^2}{\partial y^2} N_{xy}^T) \\
&+ A Q_{12} (\Phi_{,xxyy} + \frac{\partial^2}{\partial x^2} N_x^T) + A Q_{22} (\Phi_{,xxxx} + \frac{\partial^2}{\partial x^2} N_y^T) + A Q_{26} (-\Phi_{,xxyy} + \frac{\partial^2}{\partial x^2} N_{xy}^T) \\
&- A Q_{16} (\Phi_{,xyyy} + \frac{\partial^2}{\partial x \partial y} N_x^T) - A Q_{26} (\Phi_{,xxyy} + \frac{\partial^2}{\partial x \partial y} N_y^T) - A Q_{66} (-\Phi_{,xxyy} + \frac{\partial^2}{\partial x \partial y} N_{xy}^T) \\
&- (+w_{0,xy}^2 + 2w_{0,xy}^* w_{0,xy} - w_{0,xx} w_{0,yy} - w_{0,xx}^* w_{0,yy} - w_{0,xx} w_{0,yy}^*) = 0
\end{aligned} \tag{15}$$

where the matrices AQ_{ij} ($i, j = 1, 2, 6$) are given by

$$AQ = \left\{ \begin{matrix} Q_{11}^a & Q_{12}^a & 0 \\ Q_{12}^a & Q_{22}^a & 0 \\ 0 & 0 & Q_{66}^a \end{matrix} \right\} I_1 + \left\{ \begin{matrix} A_{11} & A_{12} & A_{16} \\ A_{21} & A_{22} & A_{26} \\ A_{61} & A_{62} & A_{66} \end{matrix} \right\}^{-1} \quad (16)$$

Eqs. (14) and (15) are two basic equations in terms of four variables ϕ_x , ϕ_y , w_0 , and Φ , which Eq. (15) is the same as one derived based on the classical laminated plate theory [21].

3 ANALYSIS OF EQUILIBRIUM PATH

In this study, the sandwich plate is assumed to be three types of simply supported in all edges i.e. freely movable for mechanical loading, immovable (where normal to edge displacements are prevented at boundaries) for electro-thermal loading, and freely movable in the y direction and immovable in the x direction for electro-thermo-mechanical loading as follow [7,21,34,36]

All edges are freely movable simply supported (FM):

$$\begin{aligned} x = 0, a: \quad w_0 = M_x = N_{xy} = \phi_y = P_x = 0 \\ y = 0, b: \quad w_0 = M_y = N_{xy} = \phi_x = P_y = 0 \end{aligned} \quad (17)$$

All edges are immovable simply supported (IM):

$$\begin{aligned} x = 0, a: \quad u_0 = w_0 = M_x = \phi_y = P_x = 0 \\ y = 0, b: \quad v_0 = w_0 = M_y = \phi_x = P_y = 0 \end{aligned} \quad (18)$$

Two edges are freely movable simply supported and two others are immovable simply supported (FMIM):

$$\begin{aligned} x = 0, a: \quad w_0 = M_x = N_{xy} = \phi_y = P_x = 0 \\ y = 0, b: \quad v_0 = w_0 = M_y = \phi_x = P_y = 0 \end{aligned} \quad (19)$$

with the consideration of the three cases of boundary conditions in Eqs. (17), (18), and (19), we assume the following approximate solutions for lateral displacement, imperfection, stress function, and rotations [4,27,28]

$$\begin{aligned} w_0 &= W \sin \bar{m}x \sin \bar{n}y, & \bar{m} &= \frac{m\pi}{a}, \quad \bar{n} = \frac{n\pi}{b}, \quad m, n = 1, 2, \dots \\ w^* &= \mu h \sin \bar{m}x \sin \bar{n}y, & 0 &< \mu < 1 \\ \Phi &= C_1 \cos 2\bar{m}x + C_2 \cos 2\bar{n}y + C_3 \cos 2\bar{m}x \cos 2\bar{n}y \\ &+ C_4 \sin \bar{m}x \sin \bar{n}y + \frac{1}{2} N_{x0} y^2 + \frac{1}{2} N_{y0} x^2 \\ \phi_x &= C_5 \cos \bar{m}x \sin \bar{n}y \\ \phi_y &= C_6 \sin \bar{m}x \cos \bar{n}y \end{aligned} \quad (20)$$

where m and n are number of half waves in x and y directions, respectively, W is amplitude of deflection, μ represents imperfection size, N_{x0} and N_{y0} denote pre-buckling force resultants in x and y directions, respectively.

The coefficients C_1, C_2, C_3 and C_4 can obtain with substituting Eqs. (20) into Eq. (15) as:

$$C_1 = \frac{W^2 \bar{m}^2 \bar{n}^2 + 2W \mu h \bar{m}^2 \bar{n}^2}{32A Q_{22} \bar{m}^4}, \quad C_2 = \frac{W^2 \bar{m}^2 \bar{n}^2 + 2W \mu h \bar{m}^2 \bar{n}^2}{32A Q_{11} \bar{n}^4}, \quad C_3 = C_4 = 0 \quad (21)$$

The coefficients C_5 and C_6 can obtain with employing Eqs. (4) and (10) in two last equilibrium equations in (13) and exploiting the definition of ϕ_x and ϕ_y in (20) into resulting equations as:

$$C_5 = \frac{X_6 X_2 - X_3 X_5 W}{X_1 X_5 - X_4 X_2} W, \quad C_6 = \frac{X_6 X_1 - X_3 X_4 W}{X_2 X_4 - X_5 X_1} W \quad (22)$$

where expressions of coefficients X_i ($i = 1-6$) are given in Appendix B.

Subsequently, substituting the Eq. (20) into Eq. (14) and using the Galerkin method [27,37], reveals the final form of the equilibrium equations of the piezo laminated plate as:

$$\begin{aligned} & -2C_1 \bar{m}^2 \bar{n}^2 (W + \mu h)(C_1 + C_2) - N_{x0} \bar{m}^2 (W + \mu h) - N_{y0} \bar{n}^2 (W + \mu h) \\ & + [(Q_{11}^a I_2 + D_{11}) - c_1 (Q_{11}^a I_3 + F_{11})] C_5 \bar{m}^3 + [(Q_{12}^a I_2 + D_{12}) - c_1 (Q_{12}^a I_3 + F_{12}) \\ & + 2(Q_{66}^a I_2 + D_{66}) - 2c_1 (Q_{66}^a I_3 + F_{66})] C_6 \bar{m}^2 \bar{n} - c_1 (Q_{11}^a I_3 + F_{11}) W \bar{m}^4 \\ & + [-c_1 (Q_{12}^a I_3 + F_{12}) - 4c_1 (Q_{66}^a I_3 + F_{66}) - c_1 (Q_{12}^a I_3 + F_{12})] W \bar{m}^2 \bar{n}^2 \\ & + [2(Q_{66}^a I_2 + D_{66}) - 2c_1 (Q_{66}^a I_3 + F_{66}) + (Q_{12}^a I_2 + D_{12}) - c_1 (Q_{12}^a I_3 + F_{12})] C_5 \bar{m} \bar{n}^2 \\ & - c_1 (Q_{22}^a I_3 + F_{22}) W \bar{n}^4 + [(Q_{22}^a I_2 + D_{22}) - c_1 (Q_{22}^a I_3 + F_{22})] C_6 \bar{n}^3 \\ & - K W - K W \bar{m}^2 - K W \bar{n}^2 = 0 \end{aligned} \quad (23)$$

3.1 Mechanical post buckling

The simply supported piezo laminated plate with FM boundary conditions resting on elastic foundation is assumed to be subjected uniformly distributed in-plane compressive loads P_x and P_y in x and y directions, respectively. In this type of loads and boundary conditions, the pre-buckling force resultants are [21]

$$N_{x0} = -\frac{P_x}{b}, \quad N_{y0} = -\frac{P_y}{a} \quad (24)$$

Substitution of Eq. (24) into Eq. (23) leads to closed form relation of buckling and post buckling behavior of shear deformable imperfect laminated composite plate with piezoelectric actuators on elastic foundation under in-plane compressive loads as:

$$\begin{aligned} \frac{P_x}{b} = & \frac{A Q_{22} \bar{m}^4 + A Q_{11} \bar{n}^4}{A Q_{11} A Q_{22}} \times \frac{W^2 + 2W \mu h}{16(\bar{m}^2 + R \bar{n}^2)} - \frac{X_6 X_2 - X_3 X_5}{X_1 X_5 - X_4 X_2} \frac{[(Q_{11}^a I_2 + D_{11}) - c_1 (Q_{11}^a I_3 + F_{11})] \bar{m}^3}{\bar{m}^2 + R \bar{n}^2} \frac{W}{W + \mu h} \\ & - \frac{X_6 X_1 - X_3 X_4}{X_2 X_4 - X_5 X_1} \frac{[(Q_{22}^a I_2 + D_{22}) - c_1 (Q_{22}^a I_3 + F_{22})] \bar{n}^3}{\bar{m}^2 + R \bar{n}^2} \frac{W}{W + \mu h} \\ & - \left(\frac{X_6 X_1 - X_3 X_4}{X_2 X_4 - X_5 X_1} \bar{m}^2 \bar{n} + \frac{X_6 X_2 - X_3 X_5}{X_1 X_5 - X_4 X_2} \bar{m} \bar{n}^2 \right) \\ & \frac{[(Q_{12}^a I_2 + D_{12}) - c_1 (Q_{12}^a I_3 + F_{12}) + 2(Q_{66}^a I_2 + D_{66}) - 2c_1 (Q_{66}^a I_3 + F_{66})]}{\bar{m}^2 + R \bar{n}^2} \frac{W}{W + \mu h} \\ & + \frac{c_1 [(Q_{11}^a I_3 + F_{11}) \bar{m}^4 + (Q_{22}^a I_3 + F_{22}) \bar{n}^4]}{\bar{m}^2 + R \bar{n}^2} \frac{W}{W + \mu h} \\ & + \frac{[c_1 (Q_{12}^a I_3 + F_{12}) + 4c_1 (Q_{66}^a I_3 + F_{66}) + c_1 (Q_{12}^a I_3 + F_{12})] \bar{m}^2 \bar{n}^2}{\bar{m}^2 + R \bar{n}^2} \frac{W}{W + \mu h} + \frac{K_1 + K_2 \bar{m}^2 + K_2 \bar{n}^2}{\bar{m}^2 + R \bar{n}^2} \frac{W}{W + \mu h} \end{aligned} \quad (25)$$

in which

$$R = \frac{\frac{P_y}{a}}{\frac{P_x}{b}} \quad (26)$$

3.2 Electro-thermal post buckling

The simply supported piezo laminated plate with IM boundary conditions on elastic foundation is assumed at reference temperature T_i . Then, the uniform temperature may be raised to $T_i + \Delta T$, and two piezoelectric actuators are subjected to constant applied actuator voltage in thickness direction simultaneously. Substituting temperature difference $\Theta = \Delta T$ in the thermal stress resultants in Eq. (11) and integrating results

$$\begin{Bmatrix} N_x^T \\ N_y^T \end{Bmatrix} = \Delta T \begin{Bmatrix} Q_{11}^a & Q_{12}^a & 0 \\ Q_{12}^a & Q_{22}^a & 0 \end{Bmatrix} \begin{Bmatrix} \alpha_x^a \\ \alpha_y^a \\ \alpha_{xy}^a \end{Bmatrix} I_1 + \Delta T \begin{Bmatrix} A_x^T \\ A_y^T \end{Bmatrix} \quad (27)$$

where A_x^T and A_y^T are given by

$$\begin{Bmatrix} A_x^T \\ A_y^T \end{Bmatrix} = \sum_{k=1}^N \begin{Bmatrix} \bar{Q}_{11} & \bar{Q}_{12} & \bar{Q}_{16} \\ \bar{Q}_{12} & \bar{Q}_{22} & \bar{Q}_{26} \end{Bmatrix}_k \begin{Bmatrix} \alpha_x \\ \alpha_y \\ \alpha_{xy} \end{Bmatrix}_k (z_k - z_{k-1}) \quad (28)$$

In order to access pre-buckling force resultants, with consideration of IM boundary conditions, two end-shortening relations can be written as follow [18]

$$\int_0^b \int_0^a \frac{\partial u_0}{\partial x} dx dy = 0 \quad \int_0^b \int_0^a \frac{\partial v_0}{\partial y} dx dy = 0 \quad (29)$$

From Eqs. (4) and (10) one can obtain the following expressions as:

$$\begin{aligned} \frac{\partial u_0}{\partial x} &= A Q_{11} (\Phi_{,yy} + e_{31} V_a + N_x^T) + A Q_{12} (\Phi_{,xx} + e_{32} V_a + N_y^T) - \frac{1}{2} w_{0,x}^2 - w_{0,x}^* w_{0,x} \\ \frac{\partial v_0}{\partial y} &= A Q_{12} (\Phi_{,yy} + e_{31} V_a + N_x^T) + A Q_{22} (\Phi_{,xx} + e_{32} V_a + N_y^T) - \frac{1}{2} w_{0,y}^2 - w_{0,y}^* w_{0,y} \end{aligned} \quad (30)$$

Substituting Eq. (20) into Eq. (30) and solving end-shortening relations give pre-buckling force resultants as:

$$\begin{aligned} N_{x0} &= \frac{1}{4} W \left(\frac{1}{2} W + \mu h \right) \frac{\bar{m}^2 A Q_{22} - \bar{n}^2 A Q_{12}}{A Q_{11} A Q_{22} - A Q_{12}^2} - e_{31} V_a - N_x^T \\ N_{y0} &= \frac{1}{4} W \left(\frac{1}{2} W + \mu h \right) \frac{\bar{m}^2 A Q_{12} - \bar{n}^2 A Q_{11}}{A Q_{12}^2 - A Q_{11} A Q_{22}} - e_{32} V_a - N_y^T \end{aligned} \quad (31)$$

with introduction of Eq. (31) into Eq. (23) leads to closed form relation of buckling and post buckling behavior of shear deformable imperfect laminated composite plate with piezoelectric actuators on elastic foundation under uniform temperature rise and applied actuator voltage as:

$$\begin{aligned}
\Delta T = & + \frac{2(\bar{m}^2 A Q_{22} - \bar{n}^2 A Q_{12})\bar{m}^2 + (\bar{n}^2 A Q_{11} - \bar{m}^2 A Q_{12})\bar{n}^2 + \frac{A Q_{11}\bar{n}^4 + A Q_{22}\bar{m}^4}{A Q_{11} A Q_{22} - A Q_{12}^2} + \frac{A Q_{22} A Q_{11}}{A Q_{11} A Q_{22} - A Q_{12}^2}}{[(Q_{11}^a \alpha_x^a I_1 + Q_{12}^a \alpha_y^a I_1 + A_x^T)\bar{m}^2 + (Q_{12}^a \alpha_x^a I_1 + Q_{22}^a \alpha_y^a I_1 + A_y^T)\bar{n}^2]} \frac{1}{16} (W^2 + 2W \mu h) \\
& - \frac{e_{31} \mathcal{V}_a \bar{m}^2 + e_{32} \mathcal{V}_a \bar{n}^2}{[(Q_{11}^a \alpha_x^a I_1 + Q_{12}^a \alpha_y^a I_1 + A_x^T)\bar{m}^2 + (Q_{12}^a \alpha_x^a I_1 + Q_{22}^a \alpha_y^a I_1 + A_y^T)\bar{n}^2]} \\
& - \frac{X_6 X_2 - X_3 X_5}{X_1 X_5 - X_4 X_2} \frac{[(Q_{11}^a I_2 + D_{11}) - c_1 (Q_{11}^a I_3 + F_{11})]\bar{m}^3}{[(Q_{11}^a \alpha_x^a I_1 + Q_{12}^a \alpha_y^a I_1 + A_x^T)\bar{m}^2 + (Q_{12}^a \alpha_x^a I_1 + Q_{22}^a \alpha_y^a I_1 + A_y^T)\bar{n}^2]} \frac{W}{W + \mu h} \\
& - \frac{X_6 X_1 - X_3 X_4}{X_2 X_4 - X_5 X_1} \frac{[(Q_{22}^a I_2 + D_{22}) - c_1 (Q_{22}^a I_3 + F_{22})]\bar{n}^3}{[(Q_{11}^a \alpha_x^a I_1 + Q_{12}^a \alpha_y^a I_1 + A_x^T)\bar{m}^2 + (Q_{12}^a \alpha_x^a I_1 + Q_{22}^a \alpha_y^a I_1 + A_y^T)\bar{n}^2]} \frac{W}{W + \mu h} \\
& - \left(\frac{X_6 X_1 - X_3 X_4}{X_2 X_4 - X_5 X_1} \bar{m}^2 \bar{n} + \frac{X_6 X_2 - X_3 X_5}{X_1 X_5 - X_4 X_2} \bar{m} \bar{n}^2 \right) \\
& + \frac{[(Q_{12}^a I_2 + D_{12}) - c_1 (Q_{12}^a I_3 + F_{12}) + 2(Q_{66}^a I_2 + D_{66}) - 2c_1 (Q_{66}^a I_3 + F_{66})] W}{[(Q_{11}^a \alpha_x^a I_1 + Q_{12}^a \alpha_y^a I_1 + A_x^T)\bar{m}^2 + (Q_{12}^a \alpha_x^a I_1 + Q_{22}^a \alpha_y^a I_1 + A_y^T)\bar{n}^2]} \frac{W}{W + \mu h} \\
& + \frac{c_1 (Q_{11}^a I_3 + F_{11})\bar{m}^4 + c_1 (Q_{22}^a I_3 + F_{22})\bar{n}^4}{[(Q_{11}^a \alpha_x^a I_1 + Q_{12}^a \alpha_y^a I_1 + A_x^T)\bar{m}^2 + (Q_{12}^a \alpha_x^a I_1 + Q_{22}^a \alpha_y^a I_1 + A_y^T)\bar{n}^2]} \frac{W}{W + \mu h} \\
& + \frac{[-c_1 (Q_{12}^a I_3 + F_{12}) - 4c_1 (Q_{66}^a I_3 + F_{66}) - c_1 (Q_{12}^a I_3 + F_{12})]\bar{m}^2 \bar{n}^2}{[(Q_{11}^a \alpha_x^a I_1 + Q_{12}^a \alpha_y^a I_1 + A_x^T)\bar{m}^2 + (Q_{12}^a \alpha_x^a I_1 + Q_{22}^a \alpha_y^a I_1 + A_y^T)\bar{n}^2]} \frac{W}{W + \mu h} \\
& + \frac{K_1 + K_2 \bar{m}^2 + K_2 \bar{n}^2}{[(Q_{11}^a \alpha_x^a I_1 + Q_{12}^a \alpha_y^a I_1 + A_x^T)\bar{m}^2 + (Q_{12}^a \alpha_x^a I_1 + Q_{22}^a \alpha_y^a I_1 + A_y^T)\bar{n}^2]} \frac{W}{W + \mu h}
\end{aligned} \tag{32}$$

3.3 Electro-thermo-mechanical post buckling

The simply supported piezo laminated plate resting on an elastic foundation is uniformly compressed by P_x on two movable edges $x=0, a$ and simultaneously exposed to uniform temperature rise and constant applied actuator voltage through the thickness direction. The two edges $y=0, b$ are assumed to be immovable (FMIM). In this case, the pre-buckling force resultant in x direction may be written as: $N_{x_0} = -P_x / b$. In order to obtain the pre-buckling force in y direction, an end-shortening relationship may be written (like the second of Eq. (29)), which results

$$N_{y_0} = \frac{1}{4A Q_{22}} W \bar{n}^2 \left(\frac{1}{2} W + \mu h \right) + \frac{A Q_{12}}{A Q_{22}} \frac{P_x}{b} - e_{32} \mathcal{V}_a - N_y \tag{33}$$

Substitution of Eq. (33) into Eq. (23) leads to closed form relation of buckling and post buckling behavior of shear deformable imperfect laminated composite plate with piezoelectric actuators on elastic foundation under compressive load, uniform temperature rise, and applied actuator voltage as:

$$\begin{aligned}
\frac{P_x}{b} = & \frac{AQ_{22}\bar{m}^4 + 3AQ_{11}\bar{n}^4}{AQ_{22}AQ_{11}} \frac{W^2 + 2W\mu h}{16} - \frac{[e_{32}2V_a + \Delta T(Q_{12}^a\alpha_x^a I_1 + Q_{22}^a\alpha_y^a I_1 + A_y^T)]\bar{n}^2}{\bar{m}^2 - \frac{AQ_{12}}{AQ_{22}}\bar{n}^2} \\
& - \frac{X_6X_2 - X_3X_5}{X_1X_5 - X_4X_2} \frac{[(Q_{11}^a I_2 + D_{11}) - c_1(Q_{11}^a I_3 + F_{11})]\bar{m}^3}{\bar{m}^2 - \frac{AQ_{12}}{AQ_{22}}\bar{n}^2} \frac{W}{W + \mu h} \\
& - \frac{X_6X_1 - X_3X_4}{X_2X_4 - X_5X_1} \frac{[(Q_{22}^a I_2 + D_{22}) - c_1(Q_{22}^a I_3 + F_{22})]\bar{n}^3}{\bar{m}^2 - \frac{AQ_{12}}{AQ_{22}}\bar{n}^2} \frac{W}{W + \mu h} \\
& - \left(\frac{X_6X_1 - X_3X_4}{X_2X_4 - X_5X_1} \bar{m}^2 \bar{n} + \frac{X_6X_2 - X_3X_5}{X_1X_5 - X_4X_2} \bar{m} \bar{n}^2 \right) \\
& \frac{[(Q_{12}^a I_2 + D_{12}) - c_1(Q_{12}^a I_3 + F_{12}) + 2(Q_{66}^a I_2 + D_{66}) - 2c_1(Q_{66}^a I_3 + F_{66})] W}{\bar{m}^2 - \frac{AQ_{12}}{AQ_{22}}\bar{n}^2} \frac{W}{W + \mu h} \\
& + \frac{c_1(Q_{11}^a I_3 + F_{11})\bar{m}^4 + c_1(Q_{22}^a I_3 + F_{22})\bar{n}^4}{\bar{m}^2 - \frac{AQ_{12}}{AQ_{22}}\bar{n}^2} \frac{W}{W + \mu h} \\
& - \frac{[-c_1(Q_{12}^a I_3 + F_{12}) - 4c_1(Q_{66}^a I_3 + F_{66}) - c_1(Q_{12}^a I_3 + F_{12})]\bar{m}^2 \bar{n}^2}{\bar{m}^2 - \frac{AQ_{12}}{AQ_{22}}\bar{n}^2} \frac{W}{W + \mu h} + \frac{K_1 + K_2 \bar{m}^2 + K_2 \bar{n}^2}{\bar{m}^2 - \frac{AQ_{12}}{AQ_{22}}\bar{n}^2} \frac{W}{W + \mu h}
\end{aligned} \tag{34}$$

Eq. (34) is used to determine the dependence of the in-plane compressive edge loads vs. lateral deflection (for given uniform temperature rise and voltage) and conversely, the variation of the temperature difference vs. lateral deflection (for given compressive load and voltage) can be written as:

$$\begin{aligned}
\Delta T = & + \frac{AQ_{22}\bar{m}^4 + 3AQ_{11}\bar{n}^4}{AQ_{22}AQ_{11}} \frac{1}{(Q_{12}^a\alpha_x^a I_1 + Q_{22}^a\alpha_y^a I_1 + A_y^T)\bar{n}^2} \frac{1}{16} (W^2 + 2W\mu h) + \frac{(\frac{AQ_{12}}{AQ_{22}}\bar{n}^2 - \bar{m}^2) \frac{P_x}{b} - e_{32}2V_a \bar{n}^2}{(Q_{12}^a\alpha_x^a I_1 + Q_{22}^a\alpha_y^a I_1 + A_y^T)\bar{n}^2} \\
& - \frac{X_6X_2 - X_3X_5}{X_1X_5 - X_4X_2} \frac{[(Q_{11}^a I_2 + D_{11}) - c_1(Q_{11}^a I_3 + F_{11})]\bar{m}^3}{(Q_{12}^a\alpha_x^a I_1 + Q_{22}^a\alpha_y^a I_1 + A_y^T)\bar{n}^2} \frac{W}{W + \mu h} \\
& - \frac{X_6X_1 - X_3X_4}{X_2X_4 - X_5X_1} \frac{[(Q_{22}^a I_2 + D_{22}) - c_1(Q_{22}^a I_3 + F_{22})]\bar{n}^3}{(Q_{12}^a\alpha_x^a I_1 + Q_{22}^a\alpha_y^a I_1 + A_y^T)\bar{n}^2} \frac{W}{W + \mu h} - \left(\frac{X_6X_1 - X_3X_4}{X_2X_4 - X_5X_1} \bar{m}^2 \bar{n} + \frac{X_6X_2 - X_3X_5}{X_1X_5 - X_4X_2} \bar{m} \bar{n}^2 \right) \\
& \frac{[(Q_{12}^a I_2 + D_{12}) - c_1(Q_{12}^a I_3 + F_{12}) + 2(Q_{66}^a I_2 + D_{66}) - 2c_1(Q_{66}^a I_3 + F_{66})] W}{(Q_{12}^a\alpha_x^a I_1 + Q_{22}^a\alpha_y^a I_1 + A_y^T)\bar{n}^2} \frac{W}{W + \mu h} \\
& + \frac{c_1(Q_{11}^a I_3 + F_{11})\bar{m}^4 + c_1(Q_{22}^a I_3 + F_{22})\bar{n}^4}{(Q_{12}^a\alpha_x^a I_1 + Q_{22}^a\alpha_y^a I_1 + A_y^T)\bar{n}^2} \frac{W}{W + \mu h} \\
& - \frac{[-c_1(Q_{12}^a I_3 + F_{12}) - 4c_1(Q_{66}^a I_3 + F_{66}) - c_1(Q_{12}^a I_3 + F_{12})]\bar{m}^2 \bar{n}^2}{Q_{12}^a\alpha_x^a I_1 + Q_{22}^a\alpha_y^a I_1 + A_y^T} \frac{W}{W + \mu h} + \frac{K_1 + K_2 \bar{m}^2 + K_2 \bar{n}^2}{(Q_{12}^a\alpha_x^a I_1 + Q_{22}^a\alpha_y^a I_1 + A_y^T)\bar{n}^2} \frac{W}{W + \mu h}
\end{aligned} \tag{35}$$

4 RESULTS AND DISCUSSION

The efficacy of the present fully analytical method is assessed through some simply state comparisons. In addition, some numerical examples were conducted in order to examine the effects of different characteristics on the buckling and post buckling responses. The Graphite/Epoxy is used for composite part of structure, which thermal and mechanical properties are [18,38]

$$\begin{aligned} E_{11} &= 150 \text{ GPa}, \quad E_{22} = 9 \text{ GPa} \\ G_{12} &= G_{13} = 7.1 \text{ GPa}, \quad G_{23} = 2.5 \text{ GPa}, \quad \nu_{12} = 0.3 \\ \alpha_{11} &= 1.1 \times 10^{-6} \text{ } 1/^{\circ}\text{C}, \quad \alpha_{22} = 25.2 \times 10^{-6} \text{ } 1/^{\circ}\text{C} \end{aligned} \quad (36)$$

The material properties of PZT-5A as surface mounted piezoelectric actuators are [18]

$$\begin{aligned} E_{11} &= E_{22} = 63 \text{ GPa} \\ G_{12} &= G_{13} = G_{23} = 24.2 \text{ GPa}, \quad \nu_{12} = 0.3 \\ \alpha_{11} &= \alpha_{22} = 0.9 \times 10^{-6} \text{ } 1/^{\circ}\text{C} \\ d_{31} &= d_{32} = 254 \times 10^{-12} \text{ m/V} \end{aligned} \quad (37)$$

The following dimensionless foundation parameters k_1 , k_2 have been used in this study [10]

$$k_1 = \frac{K_1 b^4}{E_{22} h^3}, \quad k_2 = \frac{K_2 b^2}{E_{22} h^3} \quad (38)$$

Here, E_{22} is a property of composite material. The comparison of the present Galerkin procedure based on HSDT of Reddy, for a FM perfect composite plate [0/90/0] with or without elastic foundation subjected to equal biaxial load ($R = 1$) is presented in Table 1.

Table 1

Comparisons of non-dimensional mechanical buckling loads $P_{scr} b/E_{22} h^3$ for [0/90/0] laminated composite plate on elastic foundation.

	Solutions:	$(k_1, k_2)=(0,0)$	$(k_1, k_2)=(100,0)$	$(k_1, k_2)=(100,10)$
$h/b=0.001, a/b=1$	Shen	14.7035	16.7299	26.7299
	Xiang et al.	14.7036	16.7300	26.7300
	Present	14.7035(1,2)*	16.7299(1,2)	26.7299(1,2)
$h/b=0.1, a/b=1$	Shen	9.9754	12.0018	22.0018
	Xiang et al.	10.2024	12.2288	22.2288
	Present	9.9754(1,2)	12.0018(1,2)	22.0018(1,2)
$h/b=0.001, a/b=2$	Shen	3.6760	10.9929	20.9930
	Xiang et al.	3.6760	10.9930	20.9930
	Present	3.6760(1,1)	10.9929(1,2)	20.9929(1,2)
$h/b=0.1, a/b=2$	Shen	3.2637	9.3743	19.3743
	Xiang et al.	3.2868	9.5904	19.5904
	Present	3.2637(1,1)	9.3743(1,2)	19.3743(1,2)

*The numbers in brackets indicate the buckling mode (m, n) .

For this example, properties of composite are: $E_{11} = 40E_{22}$, $G_{12} = G_{13} = 0.6E_{22}$, $G_{23} = 0.5E_{22}$, $\nu_{12} = 0.25$. The thickness to width ratio is 0.1 and 0.001 and thickness of piezoelectric layers is set to zero. It can be found that there is no big difference with those of Shen [4] and Xiang et al. [39]. For second example, mechanical post buckling load-deflection curve for a FM isotropic ($E = 200 \text{ GPa}$ and $\nu = 0.3$) square plate without initial imperfection subjected to uniaxial load ($R = 0$) is compared in Fig. 2 with results of Shen and Li [7]. The width to thickness ratio is 100 and thickness of piezoelectric layers is zero. As shown, the plots are similar.

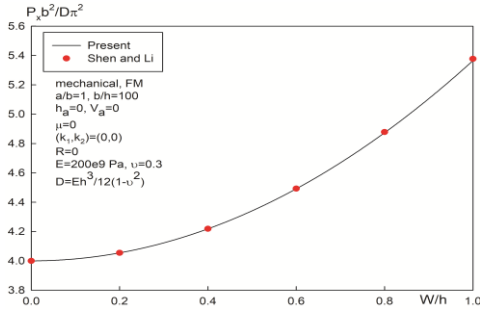


Fig.2
Comparison of mechanical post buckling paths for an isotropic plate without elastic foundation.

In order to conduct thermal loading, Table 2., shows critical temperatures for a perfect isotropic ($E = 150 \text{ GPa}$, $\nu = 0.3$, and $\alpha = 10^{-6} \text{ 1}^\circ\text{C}$) plate with IM boundary conditions, in different length to width ratios. The length to thickness ratio is 100 and thickness of piezoelectric layers is set to zero. As seen, the results are compared with first-order theory solution of Shen [40], classical theory solution of Boley and Weiner [41], finite element results of Chandrashekhara [42], and Ganapathi and Touratier [43]. In other case, thermal buckling and post buckling of a perfect isotropic plate ($E = 1\text{GPa}$, $\nu = 0.3$, and $\alpha = 10^{-6} \text{ 1}^\circ\text{C}$) with geometrical parameters $a/b = 1$, $a/h = 100$, and $h_a = 0$ and IM edges under uniform temperature rise is compared in Table 3., with results of Shen [44], Raju and Rao [1], and Kiani and Eslami [28]. As observed from Tables 2 and 3, we can conclude the method provided in this study is valid in predicting the thermal buckling and post buckling of plates.

Table 2
Comparisons of nondimensional thermal buckling loads $\alpha\Delta T_{xcr} \times 10^4$ for an isotropic plate without elastic foundation.

Solutions:	$a/b=0.25$	$a/b=0.5$	$a/b=1$	$a/b=1.5$	$a/b=2$	$a/b=2.5$	$a/b=3$
Shen	0.6720	0.7906	1.2646	2.0543	3.1589	4.5775	6.3101
Boley and Weiner	0.6722	0.7908	1.2653	2.0562	3.1633	4.5868	6.3267
Chandrashekhara	0.6727	0.7913	1.2657	2.0561	3.1617	4.5817	6.3144
Ganapathi and Touratier	0.676	0.798	1.272	2.072	3.176	4.585	6.341
Present	0.6720	0.7906	1.2646	2.0543	3.1589	4.5775	6.3089

In all cases: $(m,n)=(1,1)$

Table 3
Comparisons of non-dimensional thermal buckling and post buckling loads $\alpha\Delta T_{xcr} \times 10^4$ for an isotropic plate with Winkler elastic foundation.

k_1	Solution:	$W/h=0$	$W/h=0.2$	$W/h=0.4$	$W/h=0.6$	$W/h=0.8$	$W/h=1$
0	Shen	1.2653	1.3320	1.5330	1.8708	2.3499	2.9766
	Raju and Rao	1.2552	1.3322	1.5291	1.8681	2.3494	2.9729
	Kiani and Eslami	1.2653	1.3319	1.5318	1.8649	2.3312	2.9308
	Present	1.2646	1.3312	1.5311	1.8642	2.3305	2.9301
π^4	Shen	1.5816	1.6483	1.8494	2.1875	2.6673	3.2954
	Raju and Rao	1.5728	1.6384	1.8461	2.1852	2.6775	3.3008
	Kiani and Eslami	1.5817	1.6483	1.8481	2.1812	2.6476	3.2472
	Present	1.5809	1.6476	1.8474	2.1805	2.6469	3.2464
$\frac{2\pi^4}{10.92}$	Shen	1.8980	1.9646	2.1658	2.5041	2.9847	3.6143
	Raju and Rao	1.8900	1.9556	2.1635	2.5025	2.9947	3.6073
	Kiani and Eslami	1.8980	1.9646	2.1645	2.4976	2.9639	3.5635
	Present	1.8973	1.9639	2.1638	2.4969	2.9632	3.5628
$\frac{5\pi^4}{10.92}$	Shen	2.8470	2.9137	3.1150	3.4544	3.9379	4.5735
	Raju and Rao	2.8414	2.9071	3.1148	3.4269	3.9462	4.5586
	Kiani and Eslami	2.8470	2.9137	3.1150	3.4544	3.9379	4.5735
	Present	2.8463	2.9129	3.1128	3.4459	3.9122	4.5118

Fig. 3 gives the comparison of previous work of Bohlooly and Mirzavand [21] based on the classical laminated plate theory (CLPT) and the approach of this study using the higher-order shear deformation theory of Reddy (HSDT). Obviously, with the same geometrical and material properties for sandwich plate $[P/0/90/0/90]_s$, the electro-thermal load-deflection curves derived by HSDT are better than those by the CLPT.

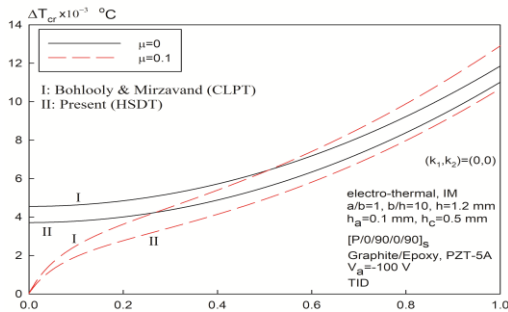


Fig.3
Comparison of thermal post buckling paths for moderately thick sandwich plate without elastic foundation.

Fig. 4 shows the difference of temperature dependency and independency of thermomechanical properties on the electro-thermal buckling curves versus a/b for piezo laminated plates. The variation of TD properties according to temperature for different types of materials can be found in different references. A simple function is linear as [21,27,45]: $P(T) = P_0(1 + P_1\Delta T)$. The constant P_0 can be put as in Eqs. (36) and (37) and constant P_1 are

$$\begin{aligned} E_{111} &= -0.0005 \\ E_{221} = G_{121} = G_{131} = G_{231} &= -0.0002 \\ \alpha_{111} = \alpha_{221} &= 0.0005 \end{aligned} \tag{39}$$

By applying an iterative method, the results are presented in Fig. 4. The IM perfect sandwich plate $[P/0/90/0/90]_s$ is subjected to uniform temperature rise and electrical loading of $V_a = -100$ V. The dimensionless foundation parameters are: $(k_1, k_2) = (300, 30)$, and the width to thickness ratio is 100, where $h_a = 0.1$ mm and $h_c = 0.5$ mm. As seen, the plot for TD material properties is lower than TID one. The reason is that, in TD algorithm, the calculation is more accurate.

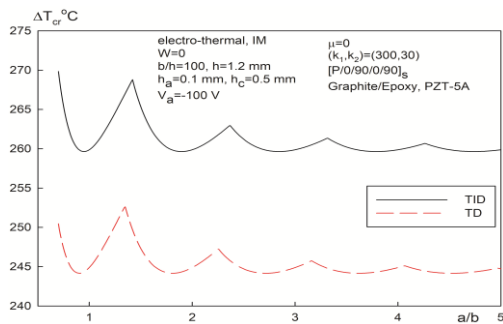


Fig.4
Effects of temperature dependency on electro-thermal buckling of the piezo laminated plate on elastic foundation.

Fig. 5 displays the mechanical buckling curves versus a/b for FM perfect sandwich plates $[P/0/90/0/90]_s$ with elastic foundation of $(k_1, k_2) = (400, 40)$ subjected to compressive loading for $R = 0, 0.5, \text{ and } 1$. As seen, for smaller values of R , the effect of modes change on the mechanical buckling response of the plate is high.

In Fig. 6, the electro-thermo-mechanical buckling curves are depicted for FMIM perfect sandwich plate $[P/0/90/0/90]_s$ rests on elastic foundation of $(k_1, k_2) = (400, 40)$ subjected to uniaxial compressive loading, uniform temperature rise of $\Delta T = 100, 200, \text{ and } 300$ °C, and electrical loading of $V_a = -100$ V. As expected, the sandwich plate under thermal loads has similar behavior with Fig. 5, which the effect of mode change in variation of critical load becomes soft with increasing of temperature.

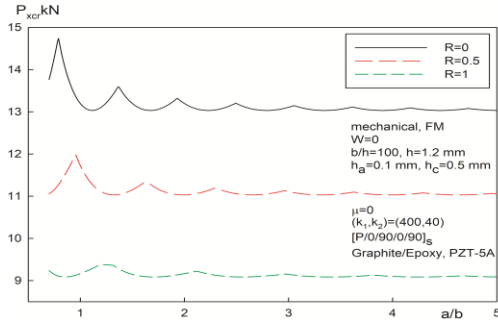


Fig.5
Effects of the ratio of compressive loads R on mechanical buckling of the piezo laminated sandwich plates on elastic foundation.

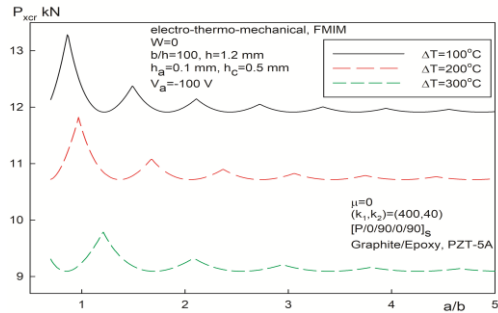


Fig.6
Effects of the uniform temperature rise on electro-thermo-mechanical buckling of the piezo laminated sandwich plates on elastic foundation.

The effects of the elastic foundations on the electro-thermal buckling of the perfect sandwich plates $[P/0/90/0/90]_s$ are depicted in Fig. 7. The IM plate is subjected to uniform temperature rise and electrical loading of $V_a = -100$ V. It can be noted that the Winkler and shear layer have good characteristics on the critical temperature especially for small values of b/h ratio.

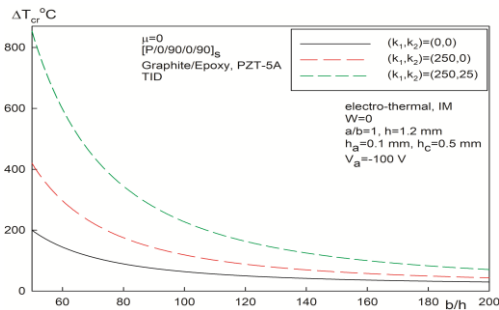


Fig.7
Effects of elastic foundation on electro-thermal buckling of the piezo laminated sandwich plates.

Fig. 8 shows the electro-thermal post buckling load-deflection curves of a piezo laminated plate resting on elastic foundation. The IM square plate $[P/0/90/0/90]_s$, with and without initial imperfection is subjected to uniform temperature rise and electrical loading of $V_a = -100$ V. The influence of Winkler and shear layer on the thermal post buckling paths are significant, where the post buckling curves for both perfect and imperfect plates become higher.

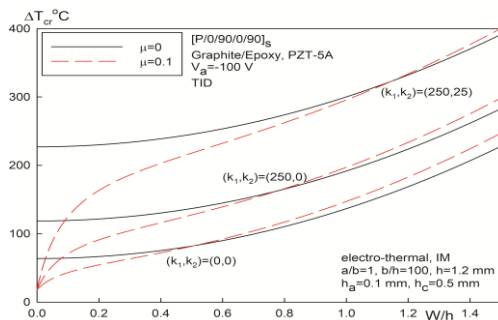


Fig.8
Effects of elastic foundation on electro-thermal post buckling of the piezo laminated sandwich plates.

Fig. 9 gives the mechanical post buckling load-deflection curves of a FM square plate $[P/0/90/0/90]_s$, with two values of initial imperfection subjected to uniaxial compression. As seen, the elastic foundation makes the plate to have higher load-deflection paths. Note that for $(k_1, k_2) = (250, 25)$, the buckling modes of both perfect and imperfect plates changes from $(m, n) = (2, 1)$ to $(m, n) = (1, 1)$ by increasing of W/h .

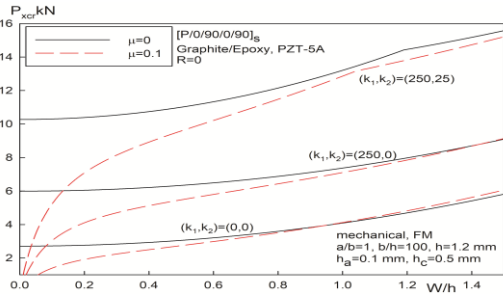


Fig.9
Effects of elastic foundation on mechanical post buckling of the piezo laminated sandwich plates.

Fig. 10 demonstrates the electro-thermo-mechanical post buckling load-deflection curves of a FMIM piezo laminated square plate $[P/0/90/0/90]_s$, with and without initial imperfection subjected to uniaxial compression, uniform temperature rise of $\Delta T = 100^\circ\text{C}$, and applied voltage $V_a = -100\text{ V}$. Obviously, the electro-thermo-mechanical post buckling paths of the plate resting on elastic foundation, for both perfect and imperfect plates are the highest curves.

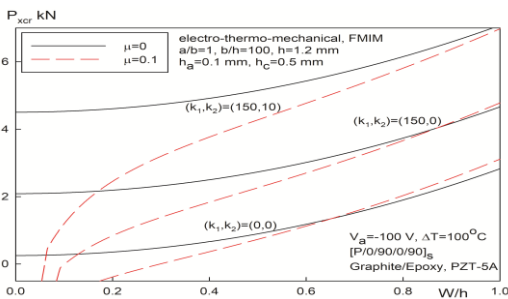


Fig.10
Effects of elastic foundation on electro-thermo-mechanical post buckling of the piezo laminated sandwich plates.

Figs. 11 and 12 represent two ways for improvement of electro-thermal buckling and post buckling of laminated composite plates as: applying negative voltages on actuators, and resting the plate on elastic foundation. The buckling behavior of IM square plate without initial imperfection in Fig. 11 and with imperfection in Fig. 12 have been improved by electrical loading of $V_a = -150, -300\text{ V}$, and elastic foundations of $(k_1, k_2) = (250, 0), (250, 25)$. As seen, for both perfect and imperfect plates, the curve of laminated composite plate with Winkler foundation is lower than the plate with surface mounted piezoelectric layers and electrical voltage of $V_a = -150\text{ V}$. In contrast, the curve of laminated composite plate with Winkler and shear layer is higher than the plate with surface mounted piezoelectric layers and electrical voltage of $V_a = -300\text{ V}$. Also as a substantial result, the imperfect curves show that, for lateral displacement of $W = 0$, elastic foundation has no effect, but by applying negative voltages on surface mounted piezoelectric actuators of sandwich plates may improve the buckling of imperfect plates.

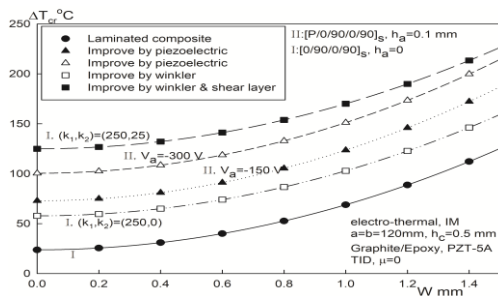


Fig.11
Improvement of electro-thermal postbuckling of the perfect plates.

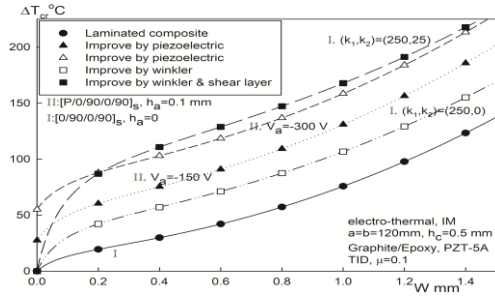


Fig.12
Improvement of electro-thermal postbuckling of the imperfect plates.

In addition, Figs. 13 and 14 shows the effects of surface mounted piezoelectric layers and elastic foundation on the electro-thermo-mechanical post buckling behavior of FMIM laminated square plate, with and without initial imperfection subjected to uniaxial compression and uniform temperature rise of $\Delta T = 40^\circ\text{C}$. As shown, they lead to broadly the same conclusions as do Figs. 11 and 12.

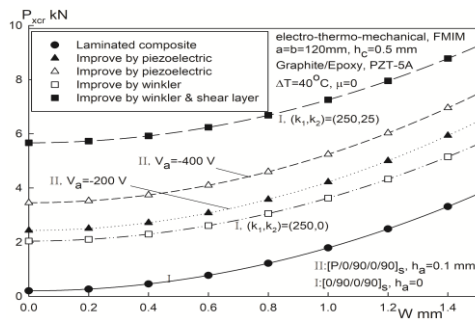


Fig.13
Improvement of electro-thermo-mechanical post buckling of the perfect plates.

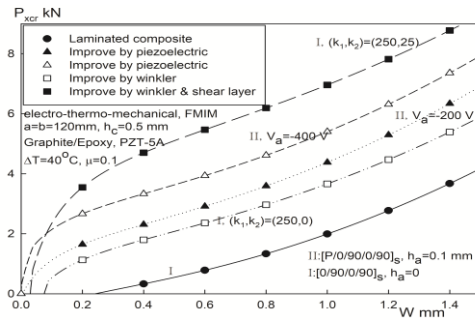


Fig.14
Improvement of electro-thermo-mechanical post buckling of the imperfect plates.

5 CONCLUSIONS

The nonlinear behavior of plates and their ability to carry loads beyond the buckling point into the post buckling range has received substantial non-analytical methods like finite element method, finite strip method, and perturbation technique. In this article, a new fully analytical method presented to introduce explicit relations for post buckling behavior of shear deformable [piezoelectric/composite/piezoelectric] plates on Pasternak type elastic foundations under different loads and boundary conditions. The closed form solutions to predicting post buckling of piezo laminated composite plates have already be done by same authors. However, for moderately and very thick plates, the results included big errors. The top features of this article are accurate calculations even for moderately thick plates by applying HSDT theory instead of past ones. Also effects of elastic foundation parameters, initial geometrical imperfections, in-plane compressive loading, temperature dependency and independency of properties, and electrical loading are discussed and as important result, in order to improve the buckling strength of perfect plates, two ways are proposed; applying suitable voltage on actuators and resting the plate on elastic foundation. In contrast, there can be exists bifurcation point for imperfect plates by applying voltage on actuators but elastic foundation has no effect.

APPENDIX A

Coefficients of thermal expansion, elastic stiffness, and piezoelectric stiffness.

$$\begin{Bmatrix} \alpha_x \\ \alpha_y \\ \alpha_{xy} \end{Bmatrix} = \begin{Bmatrix} c^2 & s^2 \\ s^2 & c^2 \\ 2cs & -2cs \end{Bmatrix} \begin{Bmatrix} \alpha_{11} \\ \alpha_{22} \end{Bmatrix}, \quad \begin{Bmatrix} \bar{Q}_{11} \\ \bar{Q}_{12} \\ \bar{Q}_{22} \\ \bar{Q}_{16} \\ \bar{Q}_{26} \\ \bar{Q}_{66} \end{Bmatrix} = \begin{Bmatrix} c^4 & 2c^2s^2 & s^4 & 4c^2s^2 \\ c^2s^2 & c^4+s^4 & c^2s^2 & -4c^2s^2 \\ s^4 & 2c^2s^2 & c^4 & 4c^2s^2 \\ c^3s & cs^3-c^3s & -cs^3 & -2cs(c^2-s^2) \\ cs^3 & c^3s-cs^3 & -c^3s & 2cs(c^2-s^2) \\ c^2s^2 & -2c^2s^2 & c^2s^2 & (c^2-s^2)^2 \end{Bmatrix} \begin{Bmatrix} Q_{11} \\ Q_{12} \\ Q_{22} \\ Q_{66} \end{Bmatrix}$$

$$\begin{Bmatrix} \bar{Q}_{44} \\ \bar{Q}_{45} \\ \bar{Q}_{55} \end{Bmatrix} = \begin{Bmatrix} c^2 & s^2 \\ -cs & cs \\ s^2 & c^2 \end{Bmatrix} \begin{Bmatrix} Q_{44} \\ Q_{55} \end{Bmatrix}, \quad Q_{11} = \frac{E_{11}}{(1-\nu_{12}\nu_{21})}, \quad Q_{22} = \frac{E_{22}}{(1-\nu_{12}\nu_{21})}, \quad Q_{12} = \frac{\nu_{21}E_{11}}{(1-\nu_{12}\nu_{21})}$$

$$Q_{44} = G_{23}, \quad Q_{55} = G_{13}, \quad Q_{66} = G_{23}, \quad \nu_{21} = \nu_{12} \frac{E_{22}}{E_{11}}, \quad c = \cos \theta, \quad s = \sin \theta$$

$$\begin{Bmatrix} e_{31} \\ e_{32} \\ e_{24} \\ e_{15} \end{Bmatrix} = \begin{Bmatrix} Q_{11}^a & Q_{12}^a & 0 & 0 \\ Q_{12}^a & Q_{22}^a & 0 & 0 \\ 0 & 0 & Q_{44}^a & 0 \\ 0 & 0 & 0 & Q_{55}^a \end{Bmatrix} \begin{Bmatrix} d_{31} \\ d_{32} \\ d_{24} \\ d_{15} \end{Bmatrix}$$

APPENDIX B

The parameters X_1 , X_2 , X_3 , X_4 , X_5 , and X_6 .

$$\begin{aligned} X_1 = & -\{[-Q_{55}^a I_1 + 3c_1 Q_{55}^a I_2 - A_{55} + 3c_1 D_{55} + 3c_1 Q_{55}^a I_2 - 9c_1^2 Q_{55}^a I_3 + 3c_1 D_{55} - 9c_1^2 F_{55}] \\ & + [Q_{11}^a I_2 - c_1 Q_{11}^a I_3 + D_{11} - c_1 F_{11} - c_1 Q_{11}^a I_3 + c_1^2 Q_{11}^a I_4 - c_1 F_{11} + c_1^2 J_{11}](-\bar{m}^2) \\ & + [Q_{66}^a I_2 - c_1 Q_{66}^a I_3 + D_{66} - c_1 F_{66} - c_1 Q_{66}^a I_3 + c_1^2 Q_{66}^a I_4 - c_1 F_{66} + c_1^2 J_{66}](-\bar{n}^2)\} \\ X_2 = X_4 = & \bar{m}\bar{n}[Q_{12}^a I_2 - c_1 Q_{12}^a I_3 + D_{12} - c_1 F_{12} + Q_{66}^a I_2 - c_1 Q_{66}^a I_3 + D_{66} - c_1 F_{66} \\ & - c_1 Q_{12}^a I_3 + c_1^2 Q_{12}^a I_4 - c_1 F_{12} + c_1^2 J_{12} - c_1 Q_{66}^a I_3 + c_1^2 Q_{66}^a I_4 - c_1 F_{66} + c_1^2 J_{66}] \\ X_3 = & [-c_1 Q_{11}^a I_3 - c_1 F_{11} + c_1^2 Q_{11}^a I_4 + c_1^2 J_{11}] \bar{m}^3 + [-c_1 Q_{12}^a I_3 - c_1 F_{12} - 2c_1 Q_{66}^a I_3 - 2c_1 F_{66} \\ & + c_1^2 Q_{12}^a I_4 + c_1^2 J_{12} + 2c_1^2 J_{66} + 2c_1^2 Q_{66}^a I_4] \bar{m}\bar{n}^2 + [-Q_{55}^a I_1 + 3c_1 Q_{55}^a I_2 - A_{55} + 3c_1 D_{55} + 3c_1 Q_{55}^a I_2 \\ & - 9c_1^2 Q_{55}^a I_3 + 3c_1 D_{55} - 9c_1^2 F_{55}](-\bar{m}) \\ X_5 = & \{[-Q_{44}^a I_1 + 3c_1 Q_{44}^a I_2 - A_{44} + 3c_1 D_{44} + 3c_1 Q_{44}^a I_2 - 9c_1^2 Q_{44}^a I_3 + 3c_1 D_{44} - 9c_1^2 F_{44}] \\ & + [Q_{66}^a I_2 - c_1 Q_{66}^a I_3 + D_{66} - c_1 F_{66} - c_1 Q_{66}^a I_3 + c_1^2 Q_{66}^a I_4 - c_1 F_{66} + c_1^2 J_{66}](\bar{m}^2) \\ & + [+I_2 Q_{22}^a - c_1 Q_{22}^a I_3 + D_{22} - c_1 F_{22} - c_1 Q_{22}^a I_3 + c_1^2 Q_{22}^a I_4 - c_1 F_{22} + c_1^2 J_{22}](\bar{n}^2)\} \\ X_6 = & [-c_1 Q_{22}^a I_3 - c_1 F_{22} + c_1^2 Q_{22}^a I_4 + c_1^2 J_{22}](\bar{n}^3) \\ & + [-2c_1 Q_{66}^a I_3 - 2c_1 F_{66} - c_1 Q_{12}^a I_3 - c_1 F_{12} + 2c_1^2 Q_{66}^a I_4 + 2c_1^2 J_{66} + c_1^2 Q_{12}^a I_4 + c_1^2 J_{12}](\bar{m}^2 \bar{n}) \\ & - [-Q_{44}^a I_1 + 3c_1 Q_{44}^a I_2 - A_{44} + 3c_1 D_{44} + 3c_1 Q_{44}^a I_2 - 9c_1^2 Q_{44}^a I_3 + 3c_1 D_{44} - 9c_1^2 F_{44}](\bar{n}) \end{aligned}$$

REFERENCES

- [1] Raju K.K., Rao G.V., 1988, Thermal post-buckling of a square plate resting on an elastic foundation by finite element method, *Computers & Structures* **28**: 195-199.

- [2] Gunda J.B., 2013, Thermal post-buckling analysis of square plates resting on elastic foundation: A simple closed-form solutions, *Applied Mathematical Modelling* **37**: 5536-5548.
- [3] De Holanda A., Gonçalves P., 2003, Postbuckling analysis of plates resting on a tensionless elastic foundation, *Journal of Engineering Mechanics* **129**: 438-448.
- [4] Shen H.-S., 2000, Postbuckling of shear deformable laminated plates under biaxial compression and lateral pressure and resting on elastic foundations, *International Journal of Mechanical Sciences* **42**: 1171-1195.
- [5] Shen H.-S., 2000, Thermomechanical postbuckling of imperfect shear deformable laminated plates on elastic foundations, *Computer Methods in Applied Mechanics* **189**: 761-784.
- [6] Shen H.-S., 2000, Postbuckling analysis of shear-deformable composite laminated plates on two-parameter elastic foundations, *Mechanics of Composite Materials and Structures* **7**: 249-268.
- [7] Shen H.-S., Li Q., 2004, Postbuckling of shear deformable laminated plates resting on a tensionless elastic foundation subjected to mechanical or thermal loading, *International Journal of Solids and Structures* **41**: 4769-4785.
- [8] Yang J., Zhang L., 2000, Nonlinear analysis of imperfect laminated thin plates under transverse and in-plane loads and resting on an elastic foundation by a semi-analytical approach, *Thin-Walled Structures* **38**: 195-227.
- [9] Singh B., Lal A., Kumar R., 2009, Post buckling response of laminated composite plate on elastic foundation with random system properties, *Communications in Nonlinear Science and Numerical Simulation* **14**: 284-300.
- [10] Singh B., Lal A., 2010, Stochastic analysis of laminated composite plates on elastic foundation: The cases of post-buckling behavior and nonlinear free vibration, *International Journal of Pressure Vessels and Piping* **87**: 559-574.
- [11] Pandey R., Shukla K., Jain A., 2009, Thermoelastic stability analysis of laminated composite plates: An analytical approach, *Communications in Nonlinear Science and Numerical Simulation* **14**: 1679-1699.
- [12] Librescu L., Stein M., 1991, A geometrically nonlinear theory of transversely isotropic laminated composite plates and its use in the post-buckling analysis, *Thin-Walled Structures* **11**: 177-201.
- [13] Noor A.K., Peters J.M., 1992, Post buckling of multilayered composite plates subjected to combined axial and thermal loads, *Finite Elements in Analysis and Design* **11**: 91-104.
- [14] Sundaresan P., Singh G., Rao G.V., 1996, Buckling and post-buckling analysis of moderately thick laminated rectangular plates, *Computers & Structures* **61**: 79-86.
- [15] Argyris J., Tenek L., 1995, Postbuckling of composite laminates under compressive load and temperature, *Computer Methods in Applied Mechanics* **128**: 49-80.
- [16] Han S.-C., Lee S.-Y., Rus G., 2006, Postbuckling analysis of laminated composite plates subjected to the combination of in-plane shear, compression and lateral loading, *International Journal of Solids and Structures* **43**: 5713-5735.
- [17] Oh I.-K., Han J.-H., Lee I., 2000, Post buckling and vibration characteristics of piezo laminated composite plate subject to thermo-piezoelectric loads, *Journal of Sound and Vibration* **233**: 19-40.
- [18] Shen H.-S., 2001, Thermal postbuckling of shear-deformable laminated plates with piezoelectric actuators, *Composites Science and Technology* **61**: 1931-1943.
- [19] Shen H.-S., 2001, Post buckling of shear deformable laminated plates with piezoelectric actuators under complex loading conditions, *International Journal of Solids and Structures* **38**: 7703-7721.
- [20] Varelis D., Saravanos D.A., 2004, Coupled buckling and postbuckling analysis of active laminated piezoelectric composite plates, *International Journal of Solids and Structures* **41**: 1519-1538.
- [21] Bohlooly M., Mirzavand B., 2015, Closed form solutions for buckling and postbuckling analysis of imperfect laminated composite plates with piezoelectric actuators, *Composites Part B: Engineering* **72**: 21-29.
- [22] Abdollahian M., Arani A.G., Barzoki A.M., Kolahchi R., Loghman A., 2013, Non-local wave propagation in embedded armchair twbnnts conveying viscous fluid using dqm, *Physica B: Condensed Matter* **418**: 1-15.
- [23] Arani A.G., Abdollahian M., Kolahchi R., Rahmati A., 2013, Electro-thermo-torsional buckling of an embedded armchair dwbnnt using nonlocal shear deformable shell model, *Composites Part B: Engineering* **51**: 291-299.
- [24] Arani A.G., Abdollahian M., Jalaei M., 2015, Vibration of bio liquid-filled microtubules embedded in cytoplasm including surface effects using modified couple stress theory, *Journal of Theoretical Biology* **367**: 29-38.
- [25] Arani A.G., Abdollahian M., Kolahchi R., 2015, Nonlinear vibration of embedded smart composite microtube conveying fluid based on modified couple stress theory, *Polymer Composites* **36**: 1314-1324.
- [26] Bohlooly M., Mirzavand B., 2018, Postbuckling and deflection response of imperfect piezo-composite plates resting on elastic foundations under in-plane and lateral compression and electro-thermal loading, *Mechanics of Advanced Materials Structures* **25**: 192-201.
- [27] Mirzavand B., Bohlooly M., 2015, Thermal buckling of piezolaminated plates subjected to different loading conditions, *Journal of Thermal Stresses* **38**: 1138-1162.
- [28] Kiani Y., Eslami M., 2012, Thermal buckling and post-buckling response of imperfect temperature-dependent sandwich fgm plates resting on elastic foundation, *Archive of Applied Mechanics* **82**: 891-905.
- [29] Duc N.D., Van Tung H., 2011, Mechanical and thermal post buckling of higher order shear deformable functionally graded plates on elastic foundations, *Composite Structures* **93**: 2874-2881.
- [30] Malekzadeh K., Khalili S., Abbaspour P., 2010, Vibration of non-ideal simply supported laminated plate on an elastic foundation subjected to in-plane stresses, *Composite Structures* **92**: 1478-1484.
- [31] Joubaneh E.F., Mojahedin A., Khorshidvand A., Jabbari M., 2014, Thermal buckling analysis of porous circular plate with piezoelectric sensor-actuator layers under uniform thermal load, *Journal of Sandwich Structures & Materials* **17**: 3-25.

- [32] Reddy J.N., 2004, *Mechanics of Laminated Composite Plates and Shells: Theory and Analysis*, CRC press.
- [33] Duc N.D., Cong P.H., 2013, Nonlinear post buckling of symmetric s-fgm plates resting on elastic foundations using higher order shear deformation plate theory in thermal environments, *Composite Structures* **100**: 566-574.
- [34] Duc N.D., Cong P.H., 2014, Nonlinear post buckling of an eccentrically stiffened thin fgm plate resting on elastic foundations in thermal environments, *Thin-Walled Structures* **75**: 103-112.
- [35] Van Tung H., Duc N.D., 2010, Nonlinear analysis of stability for functionally graded plates under mechanical and thermal loads, *Composite Structures* **92**: 1184-1191.
- [36] Wang Z.-X., Shen H.-S., 2011, Nonlinear analysis of sandwich plates with FGM face sheets resting on elastic foundations, *Composite Structures* **93**: 2521-2532.
- [37] Ninh D.G., Bich D.H., 2016, Nonlinear torsional buckling and post-buckling of eccentrically stiffened ceramic functionally graded material metal layer cylindrical shell surrounded by elastic foundation subjected to thermo-mechanical load, *Journal of Sandwich Structures & Materials* **18**: 712-738.
- [38] Bohlooly M., Mirzavand B., 2017, Thermomechanical buckling of hybrid cross-ply laminated rectangular plates, *Advanced Composite Materials* **26**: 407-426.
- [39] Xiang Y., Kitipornchai S., Liew K., 1996, Buckling and vibration of thick laminates on Pasternak foundations, *Journal of Engineering Mechanics* **122**: 54-63.
- [40] Shen H.-S., 2000, Nonlinear analysis of simply supported reissner–mindlin plates subjected to lateral pressure and thermal loading and resting on two-parameter elastic foundations, *Engineering Structures* **22**: 1481-1493.
- [41] Boley B.A., Weiner J.H., 2012, *Theory of Thermal Stresses*, Courier Dover Publications.
- [42] Chandrashekhara K., 1992, Thermal buckling of laminated plates using a shear flexible finite element, *Finite Elements in Analysis and Design* **12**: 51-61.
- [43] Ganapathi M., Touratier M., 1997, A study on thermal postbuckling behaviour of laminated composite plates using a shear-flexible finite element, *Finite Elements in Analysis and Design* **28**: 115-135.
- [44] Shen H.-S., 1997, Thermal post-buckling analysis of imperfect shear-deformable plates on two-parameter elastic foundations, *Composite Structures* **63**: 1187-1193.
- [45] Mirzavand B., Eslami M., Reddy J., 2013, Dynamic thermal postbuckling analysis of shear deformable piezoelectric-fgm cylindrical shells, *Journal of Thermal Stresses* **36**: 189-206.